

Cell Reports Methods, Volume 3

Supplemental information

**CartoCell, a high-content pipeline for 3D image
analysis, unveils cell morphology
patterns in epithelia**

Jesús A. Andrés-San Román, Carmen Gordillo-Vázquez, Daniel Franco-Barranco, Laura Morato, Cecilia H. Fernández-Espartero, Gabriel Baonza, Antonio Tagua, Pablo Vicente-Munuera, Ana M. Palacios, María P. Gavilán, Fernando Martín-Belmonte, Valentina Annese, Pedro Gómez-Gálvez, Ignacio Arganda-Carreras, and Luis M. Escudero

3D ResU-Net

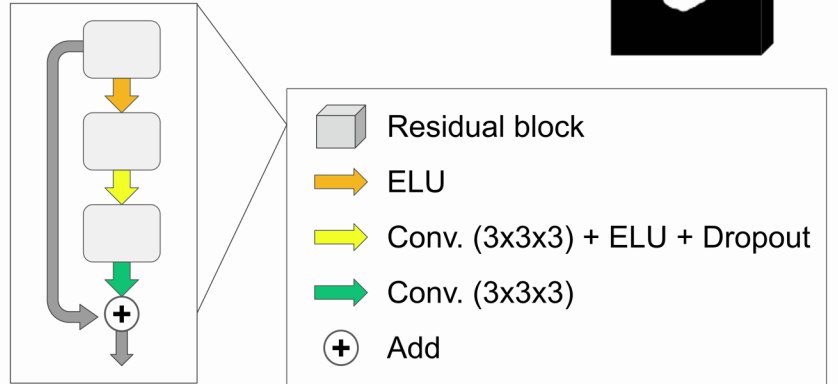
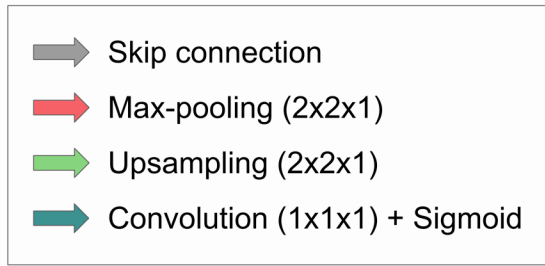
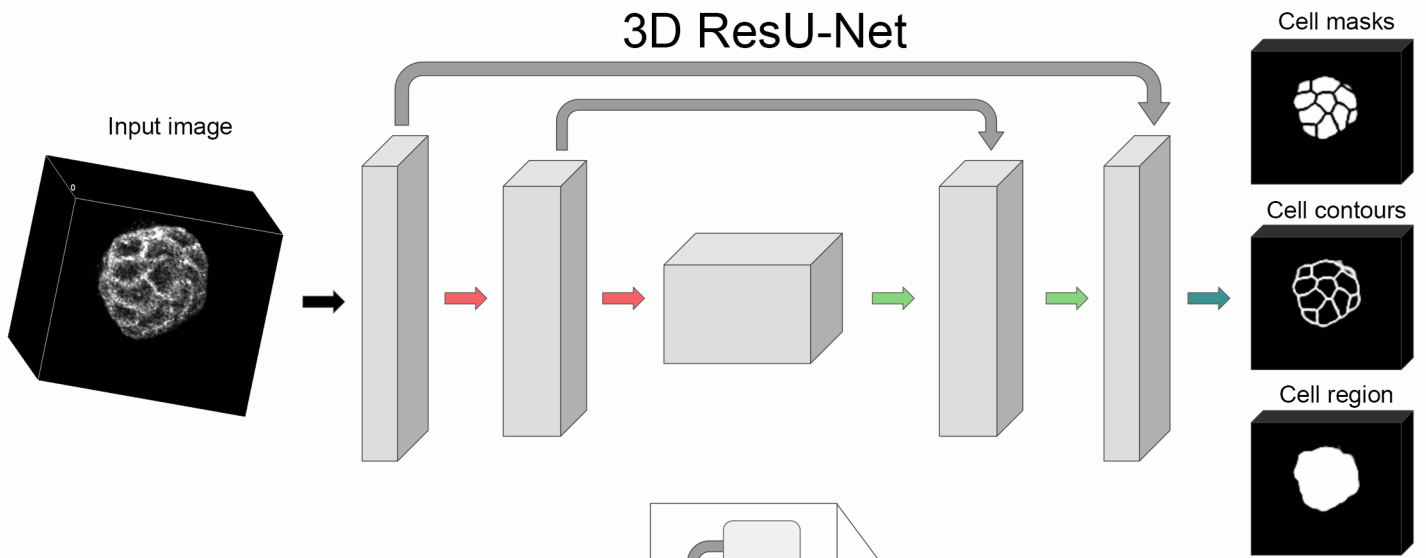
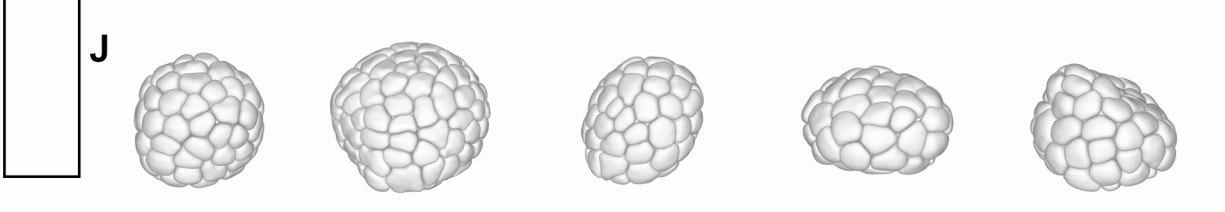
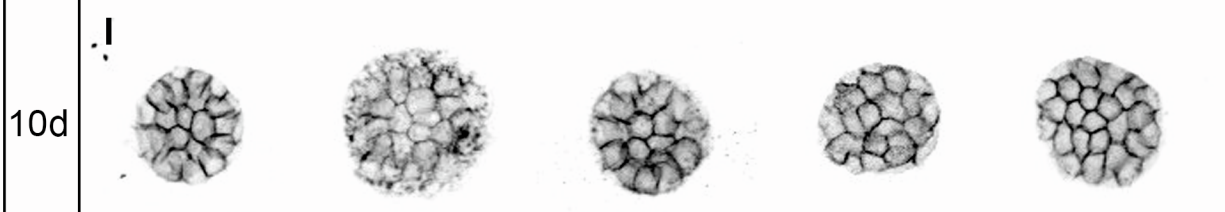
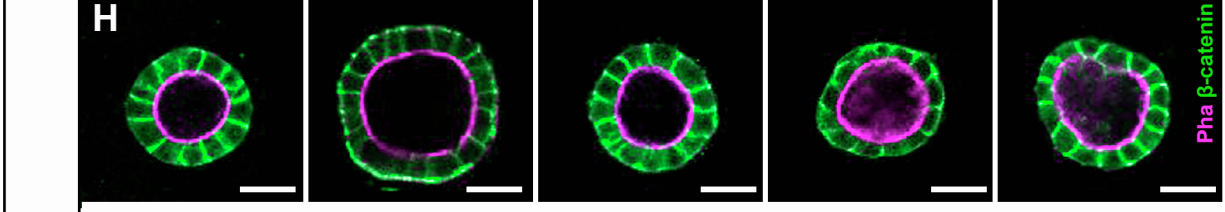
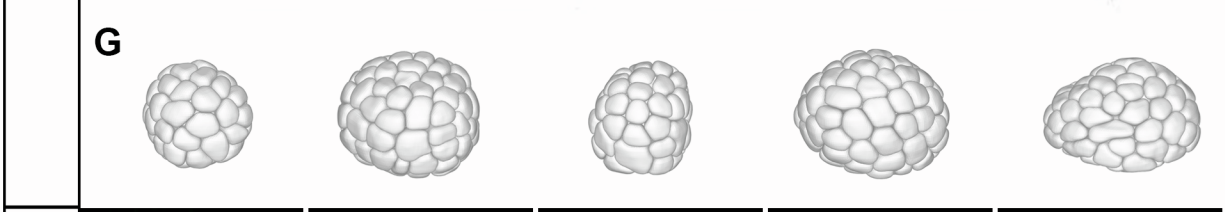
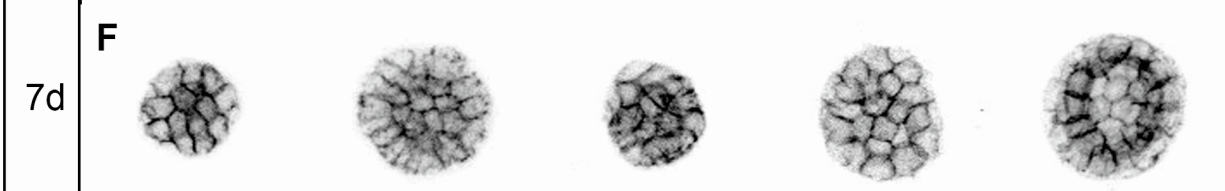
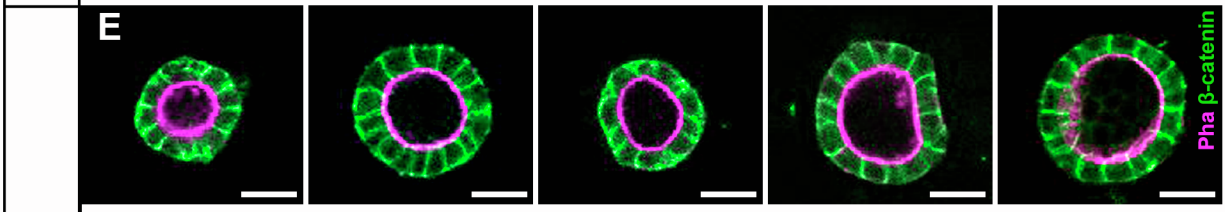
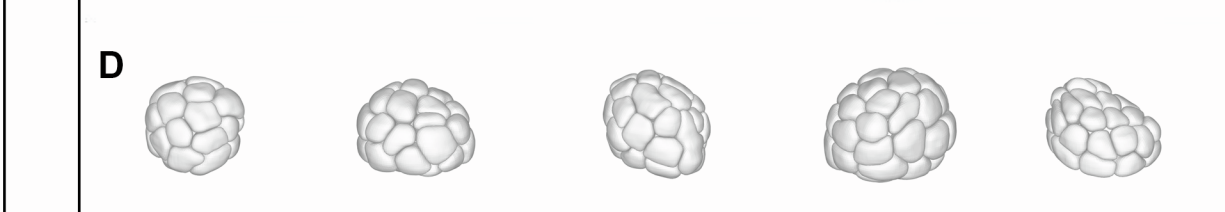
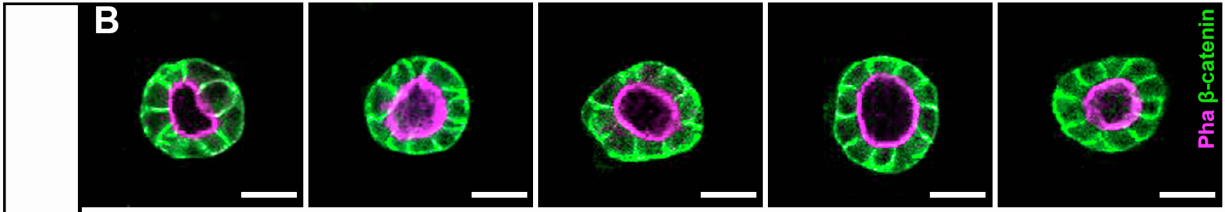
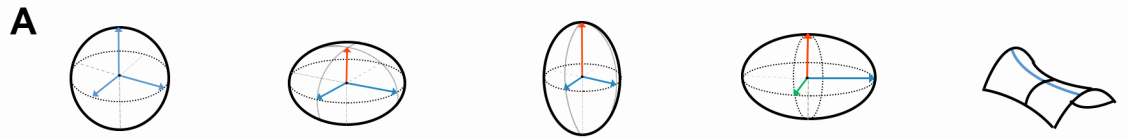


Figure S1. Architecture of the 3D ResU-Net segmentation network, Related to Figure 1.

Our proposed 3D ResU-Net is a U-Net-like network with three depth levels and residual blocks. It receives 3D single-channel images as input and produces three different outputs representing the probabilities of the individual cell masks, contours and whole cell region. Convolutional filters are applied in 3D, while the down-sampling and up-sampling operations are only performed in 2D due to the anisotropy of image data.

Sphere	Oblate	Prolate	Ellipsoid	Negative Curvature
--------	--------	---------	-----------	--------------------



Pha β -catenin

Pha β -catenin

Pha β -catenin

Figure S2. MDCK cysts adopt different shapes in 3D cell cultures, Related to Figure 1.

A) Schematic representation of the morphological cyst classification. **B, E, H)** Middle sections of top-to-bottom confocal microscopy Z-stack images of representative cysts belonging to each morphological category at 4, 7 and 10 days. Cell contours were stained with Alexa Fluor 647 phalloidin (magenta) and anti- β -catenin antibody (green) (**STAR Methods**). Scale bars, 20 μm . **C, F, I)** Half projections of representative cysts belonging to each morphological category at 4, 7 and 10 days (cell contours stained by Alexa Fluor 647 phalloidin and anti- β -catenin antibody) (**STAR Methods**). **D, G, J)** Computer rendering (front or back view) of the segmented cysts belonging to each morphological category at 4, 7 and 10 days.

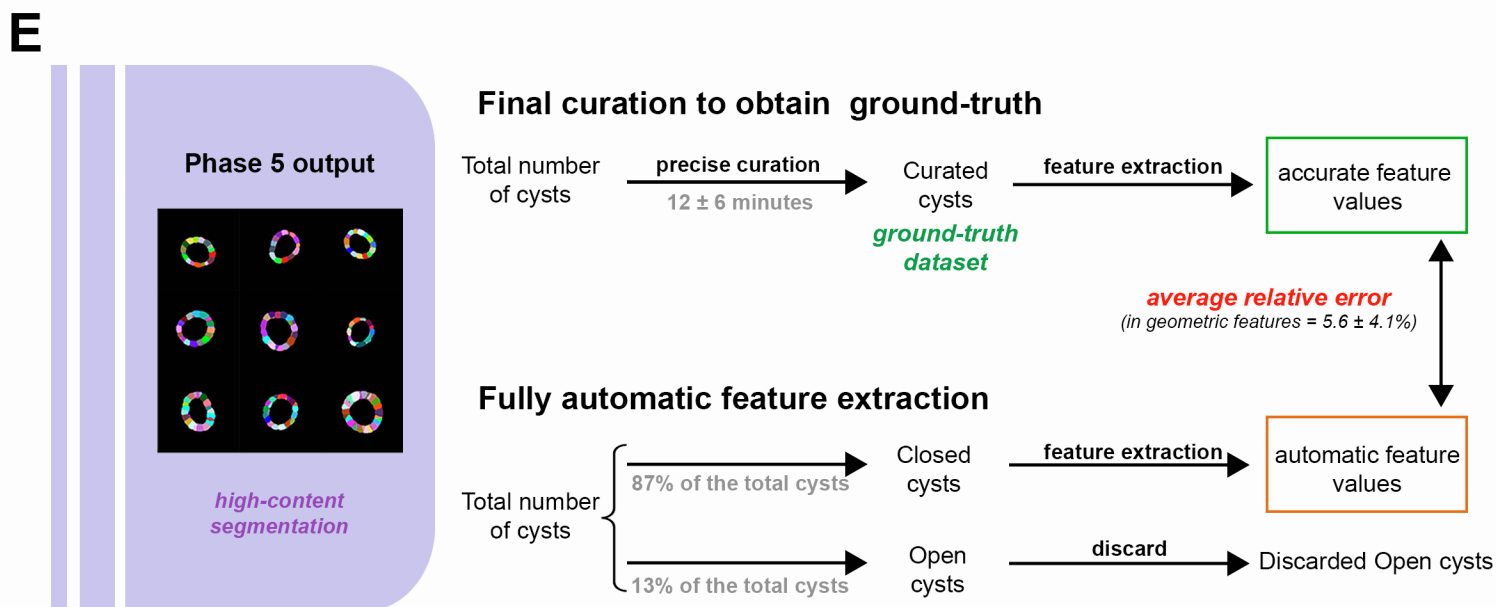
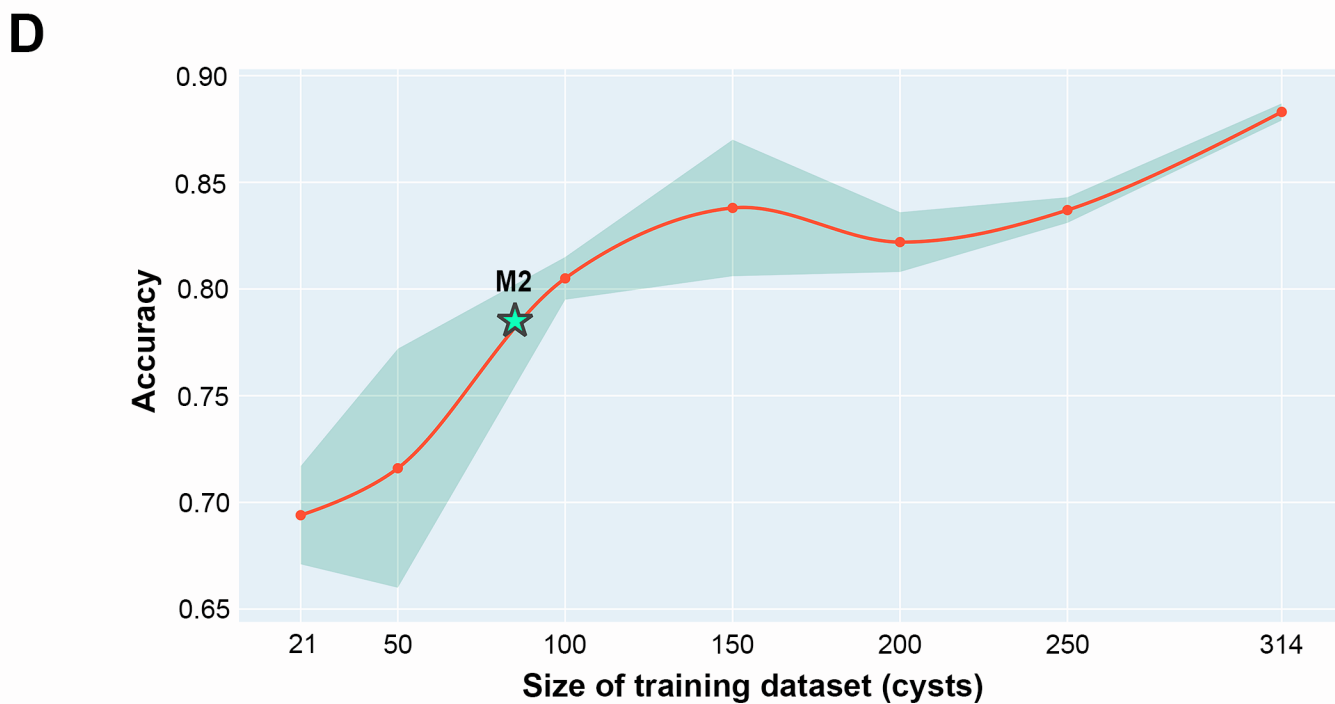
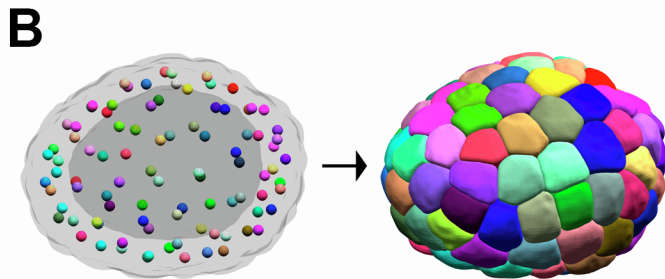
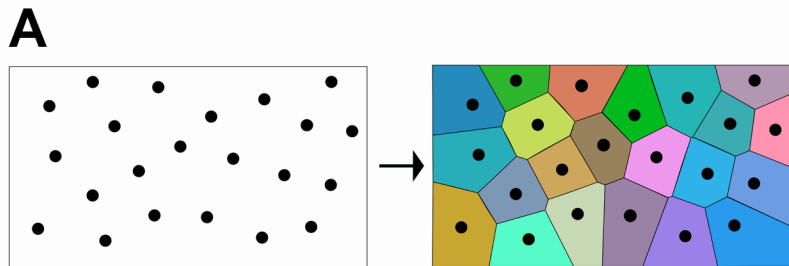
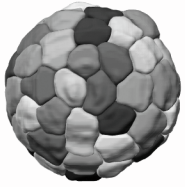


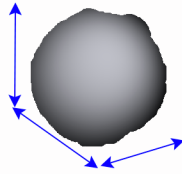
Figure S3. Appendixes and details regarding Figure 1, Related to Figure 1.

A-C) Voronoi tessellations and comparison of custom three-dimensional Voronoi based model against state-of-the-art methods. **A)** Voronoi tessellation in two dimensions occupying the space of a rectangle using randomly distributed seeds. **B)** Three-dimensional Voronoi tessellation of a cyst filling the space determined by the cell tissue using the centroids of each cell as seeds. **C)** Comparison of a manually labeled cyst (ground-truth) against our proposed method (CartoCell) and the three state-of-the-art methods chosen for comparison: PlantSeg, StarDist and Cellpose. **D)** Plot illustrating the relationship between the accuracy of a 3D ResU-Net model (y-axis), when trained with different number of perfectly annotated cysts (x-axis). The accuracy is measured for seven different dataset sizes: 21 (size of the dataset used to train the model M1), 50, 100, 150, 200, 250, and 314 (size of the imperfect dataset used to train the model M2). Each of these training scenarios is repeated 10 times to obtain the mean value (red dots) and standard deviation (blue band). The intersection between the accuracy trendline (red line) as the training dataset size increases, and the accuracy of the CartoCell model M2 is represented by a star symbol. This intersection indicated that around 90 fully segmented cysts are required in a single phase of training to achieve equivalent results to the whole pipeline of CartoCell with only 21 cysts as input. **E)** Appendix to Fig.1 showing two possible paths for feature extraction. After the Phase 5, a ground-truth dataset can be obtained by final manual curation of the results (12.0 ± 6 minutes per cyst) to extract the accurate feature values. On the other hand, there is an alternative option, opting for the automatic feature extraction of geometric data assuming an average relative error: Based on the data of our study, 46 of 353 cysts (13%) presented under-segmentation defects which induced open cysts and impaired the feature extraction. The extraction of the features of the remaining cyst (87%, closed cysts) provided results with an average error of $5.6 \pm 4.1\%$ in geometric characteristics compared with the accurate feature values (**Table S4** and **STAR Methods**).

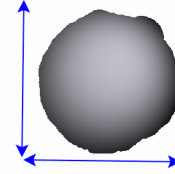
Cyst geometric features



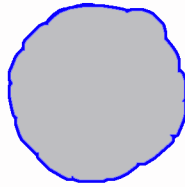
Total Cell Number



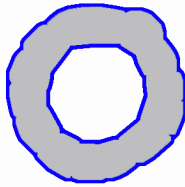
Cyst Axes Length (μm)
Length of the three axes of symmetry (major, minor and intermediate)



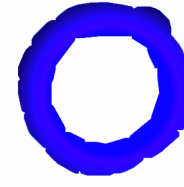
Aspect Ratio
Major axis divided by minor axis length



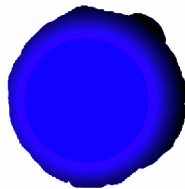
Cyst Surface Area (μm^2)
Outer surface area of the cyst



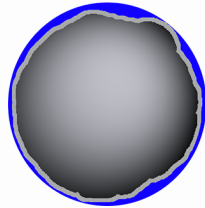
Surface Ratio
Ratio of outer surface to inner surface of the cyst



Epithelium Volume (μm^3)
Cyst volume that cells occupy

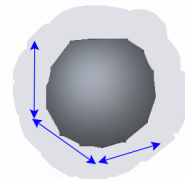


Cyst Volume (μm^3)

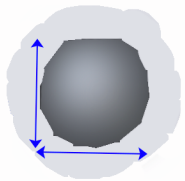


Cyst solidity
Cyst volume divided by the convex hull volume

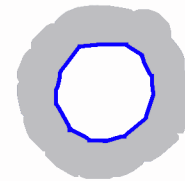
Lumen geometric features



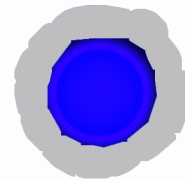
Lumen Axes Length (μm)
Length of the three axes of symmetry



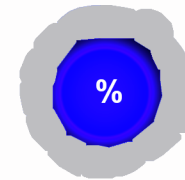
Lumen Aspect Ratio
Major lumen axis divided by minor lumen axis length



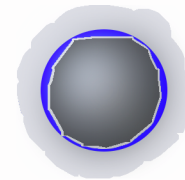
Lumen Surface Area (μm^2)



Lumen Volume (μm^3)

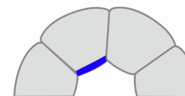


Lumen Space
Percentage of the cyst volume that the lumen occupies

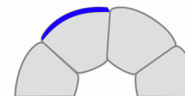


Lumen Solidity
Lumen volume divided by the convex hull volume

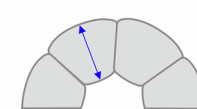
Cell geometric features



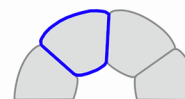
Cell Apical Area (μm^2)
Inner cell surface area



Cell Basal Area (μm^2)
Outer cell surface area



Cell Height (μm)



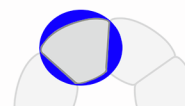
Cell Surface Area (μm^2)



Cell Volume (μm^3)



Cell Aspect Ratio
Major cell axis divided by minor cell axis length

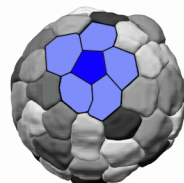


Cell Solidity
Cell volume divided by the convex hull volume

Cell packing features



Scutoids (%)
Percentage of scutoids per cyst



Total 3D Neighbors
Number of total neighboring cells of each cell

Figure S4. Qualitative definition of the geometric and packing features describing the cyst architecture, Related to Figure 2.

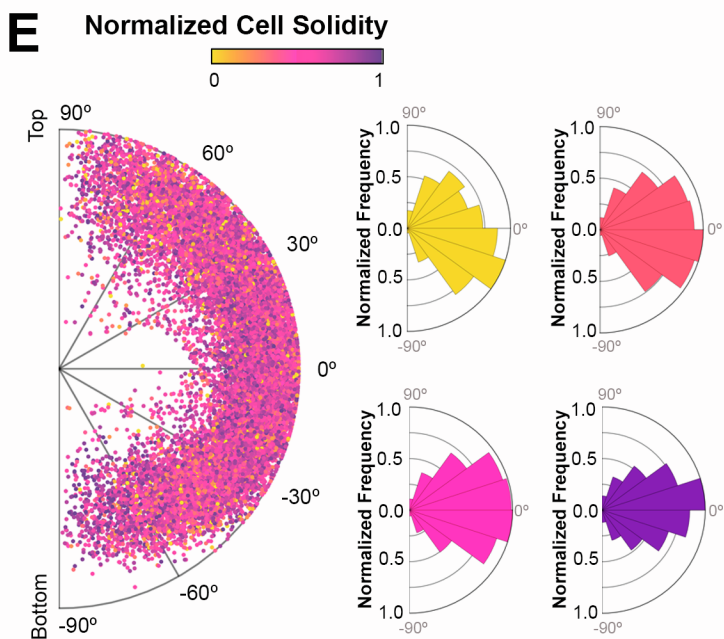
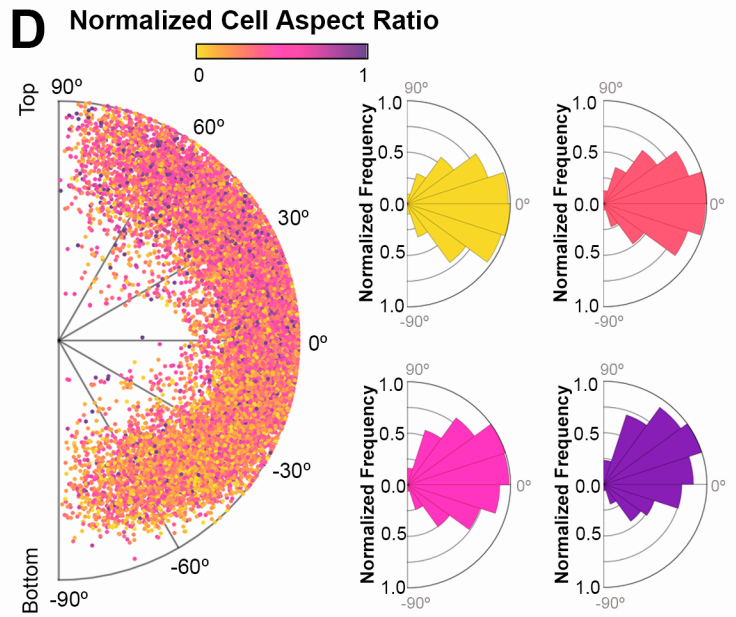
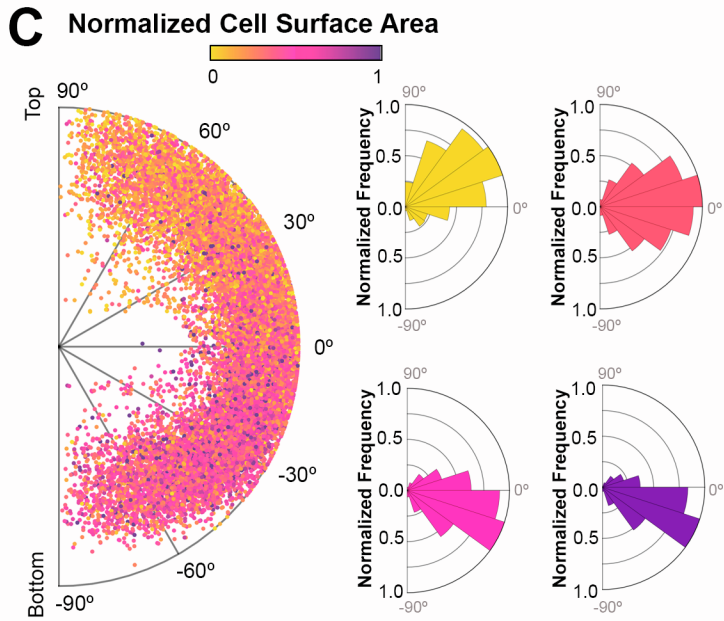
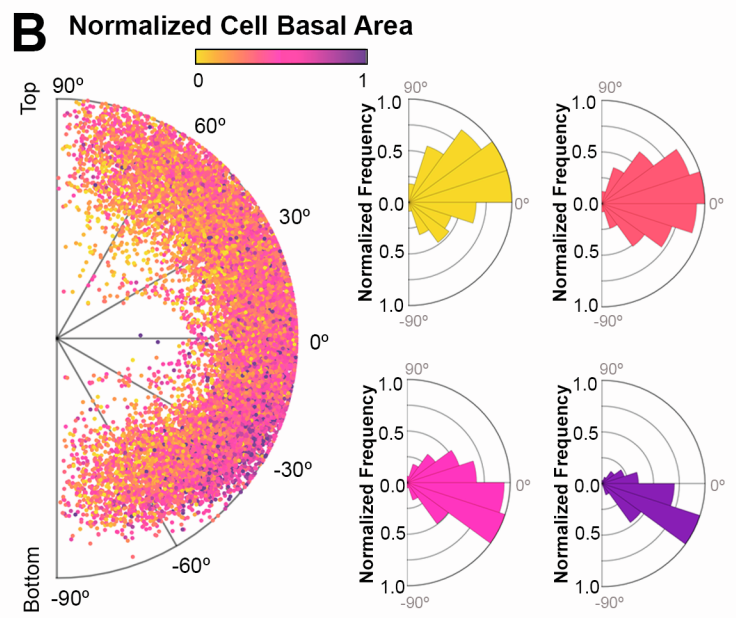
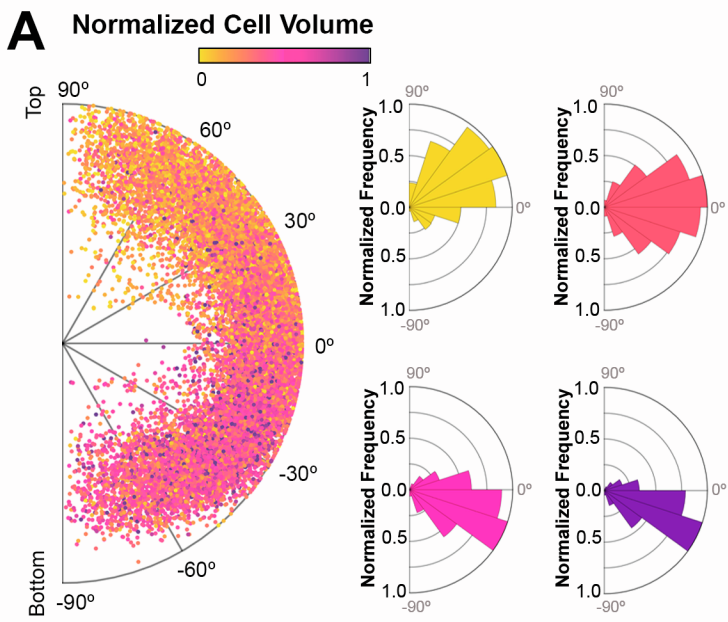


Figure S5. Examples of spatial patterns in the distribution of geometric feature values, Related to Figure 2.

Same representations as **Fig. 2E, 2G** to map the features: cell volume (**A**), cell basal area (**B**), cell surface area (**C**), cell aspect ratio (**D**) and cell solidity (**E**).

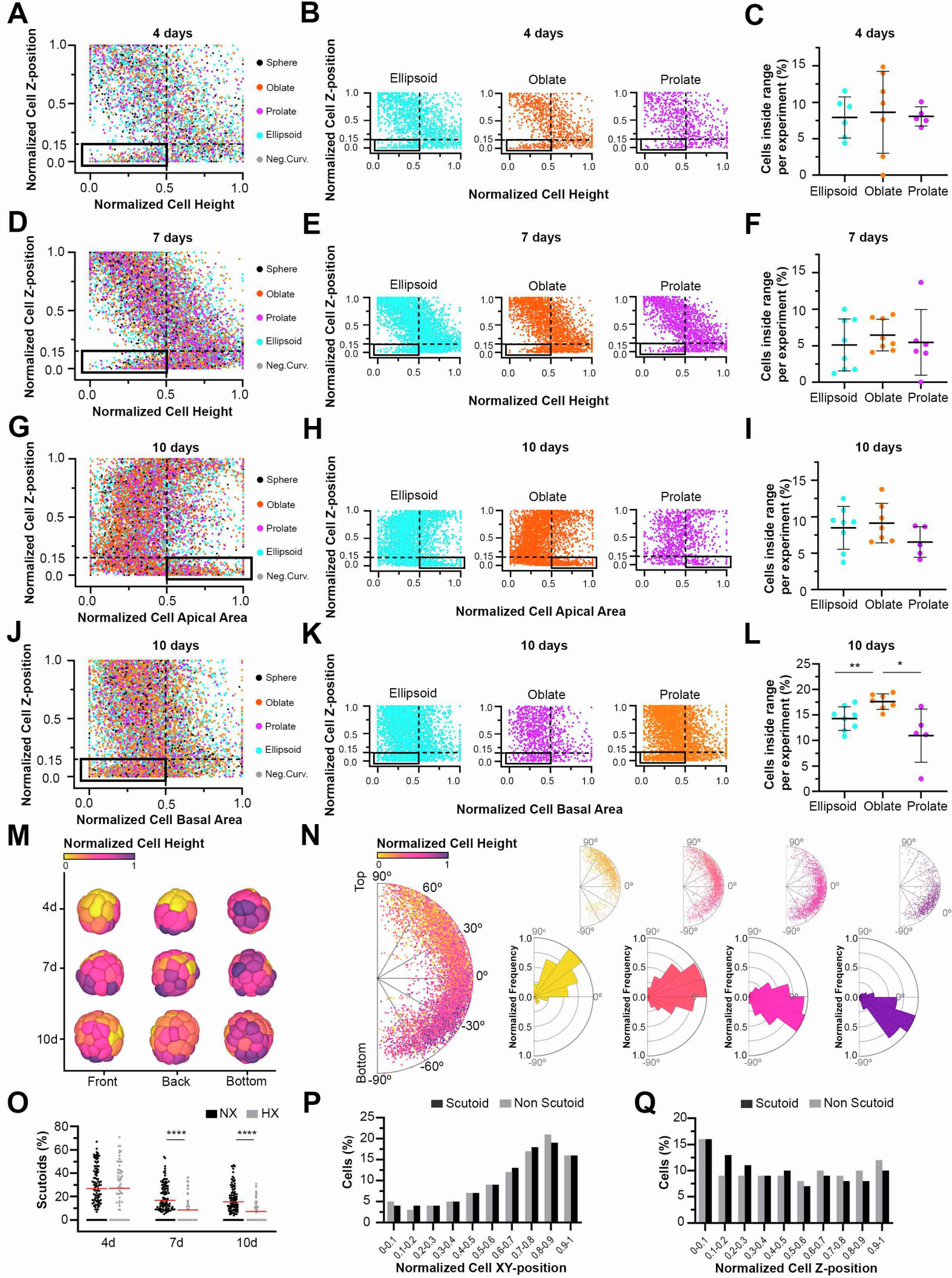


Figure S6. The cyst morphology and the hypoxia can affect the cartography of cell geometric features, Related to Figure 2 and Figure 3.

A-L) The cyst morphology affects the cartography of cell geometric features. Same representations as **Fig. 2H-2J** to explore the cell Z-position versus cell height at 4-day (**A-C**) and 7-day cysts (**D-F**), cell apical area at 10-day cysts (**G-I**) and cell basal area at 10-day cysts (**J-L**). **M-Q)** Hypoxia can induce cell morphology patterns changes in MDCK cysts. **M, N)** Same representations as **Fig. 2D-2G** to map the feature “cell height” in hypoxic (1% O₂) MDCK cysts. 7729 cells from 206 segmented cysts were represented. **O)** Scatterplots for quantification of the percentage of scutoids per cyst in normoxic (NX, black) and hypoxic (1% O₂) (HX, grey) cysts at 4, 7 and 10 days. The red bar represents the average of the dataset. Data from more than 60 segmented cysts at each time point, from at least 3 independent experiments. “*****” indicates $p \leq 0.0001$ (Mann-Whitney U test). **P, Q)** Same representations as **Fig. 2L, 2M** to map the scutoidal (black) and non-scutoidal (grey) cells along XY (**P**) and Z axes (**Q**) in hypoxic (1% O₂) cysts. Percentage of all cells from the 206 segmented hypoxic cysts.